


Dy³⁺ ions in fluorophosphate glasses for luminescent white light applications

K Venkata Rao^{1,*} , S Vidya Sagar^{1,2}, N V Srihari³ and Sanjay J Dhoble⁴

¹ Department of Physics, Govt. Degree College, Porumamilla, Kadapa, A.P 516193, India

² Department of Physics, Yogi Vemana University, Kadapa, A.P 516005, India

³ Department of Physics, Govt. Degree College, Kandukur, A.P 523105, India

⁴ Department of Physics, RTM Nagpur University, Nagpur, Maharashtra 440033, India

E-mail: drvenkatarao@gmail.com

Received 19 April 2024, revised 11 October 2024

Accepted for publication 23 October 2024

Published 1 November 2024



CrossMark

Abstract

In this study, a series of fluorophosphate (FP) glasses, activated with Dy³⁺ ions and displaying concentration dependence, have been prepared and analysed for their suitability in luminescent white light applications. The melt quenching method was utilized to fabricate a set of FP glasses, doped with Dy³⁺ ions and possessing the composition of (60 - x) P₂O₅ + 10MgO + 10ZnO + 10BiF₃ + 10KF + xDy₂O₃, where x ranges from 0.1 to 2.0 mol%. The structural properties of the samples were analysed using x-ray diffraction (XRD), scanning electron microscope (SEM), Fourier transform infrared (FTIR), and Raman spectroscopy while the optical properties of the samples were studied using absorption and emission spectra. The amorphous nature of the FP glasses was confirmed through SEM analysis and XRD profiles. Moreover, the presence of elements in their composition was verified using EDX. The FTIR spectra of the FP glasses exhibited vibration bands consistent with the characteristic phosphate groups, which was further supported by Raman analysis. The absorption spectra were used to calculate oscillator strengths (f_{exp} & f_{cal}) and Judd–Ofelt (JO) parameters Ω_{λ} ($\lambda = 2, 4, 6$). The values of Ω_{λ} ($\lambda = 2, 4, 6$) followed this order: $\Omega_6 > \Omega_2 > \Omega_4$. The emission spectra displayed three prominent transitions in the UV–visible region: (⁴F_{9/2} → ⁶H_{15/2}) blue, (⁴F_{9/2} → ⁶H_{13/2}) yellow, and (⁴F_{9/2} → ⁶H_{11/2}) red. The peak at 553 nm (⁴F_{9/2} → ⁶H_{13/2}) was the most intense and dominant. Radiative characteristics were evaluated from the emission spectra through the employment of JO intensity parameters and refractive indices. The Y/B intensity ratio values were greater than 1, indicating the high covalency of Dy³⁺ ions. The colour coordinates (x, y) and correlated colour temperature values of CIE 1931 were situated in the cool white region. The comprehensive analysis suggests that these glasses have the potential to become highly favourable candidates as luminescent components for solid-state white light emitting instruments.

Keywords: Dy³⁺ glass, fluorophosphate (FP) glass, JO parameters, absorption spectra, emission spectra

* Author to whom any correspondence should be addressed.

1. Introduction

In present-day materials science and photonics, considerable efforts have been made to produce effective and versatile light-producing gadgets, prompting earth-shattering headways. Dy³⁺ ion-containing fluorophosphate (FP) glasses are a prominent type of device that has emerged as a remarkable approach for the realisation of white-light emission devices in the fields of modern materials science and photonics.

For optical applications, phosphate glasses must contain fluorine as the starting material to act as a host for luminescent rare-earth ions and have the desired optical properties of fluoride glasses and superior mechanical and thermal stability of phosphate glasses [1]. These glasses offer a high degree of chemical stability, low melting point, notable moisture resistance, relatively low refractive index, and relatively low phonon energy, and are known for their high transparency in the UV spectrum [1–3] and low optical basicity [3]. Fluoride phosphate and FP glasses represent a fascinating foundation for various applications in optics, photonics, and energy storage [3].

The sharp emission bands of dysprosium (Dy³⁺) ions allow their use in laser devices and commercial displays [4]. Its presence in doped glasses is important for the creation of white LEDs, which can replace traditional light sources [4]. Among the various RE³⁺ ions, Dy³⁺ is an excellent optical activator [5], emitting simultaneous (blue: $^4F_{9/2} \rightarrow ^6H_{15/2}$), (yellow: $^4F_{9/2} \rightarrow ^6H_{13/2}$), and (red: $^4F_{9/2} \rightarrow ^6H_{11/2}$) emissions, which are useful for laser action and optical amplification [6]. Optimising the local field around Dy³⁺ ions with yellow-to-blue (Y/B) intensity ratio is crucial for white-light emission [4, 7, 8]. In this study, phosphate glasses doped with Dy³⁺ ions were investigated by modifying their phosphate networks using KF and BiF₃. The chemical instability of phosphates owing to their P–O–P bonds can be addressed by incorporating multivalent oxide network formers, such as ZnO and MgO, which function as effective glass modifiers [9]. The appropriate selection of a glass modifier may mitigate the quenching effect of Dy³⁺ emissions [10].

Recently, a significant amount of scholarly enquiry has been conducted on different glass matrices doped with Dy³⁺ ions. Rasool *et al* conducted a thorough investigation of the spectroscopic properties of concentration-dependent Dy³⁺ ion-doped B₂O₃–CaO–NaF glasses, with the possibility of utilising them as white LEDs [11]. Kashif and Ratep conducted a study on the development of zinc borotellurite glasses doped with various concentrations of dysprosium oxide, focusing on their optical and physical properties for potential applications in optoelectronics [12]. Another study by Kuwik *et al* investigated the spectral properties of lead-free borate glasses doped with trivalent Dy³⁺ ions and the influence of glass formers and glass modifiers on these properties [13]. This study showed that these glasses exhibit visible luminescence and have the potential to be used as yellowish emitters. Abdullahi *et al* found that incorporating CuO nanoparticles into a trivalent Dy³⁺ ion-doped multicomponent telluroborate glass matrix improved the up-conversion

emission and nonlinear optical characteristics [14]. Bairagi *et al* examined the optical and photoluminescence properties of trivalent Dy³⁺-ion-doped zinc sodium tellurite glass [15]. The current investigation focuses on FP glasses that have been infused with Dy³⁺ ions and have been subjected to a comprehensive examination to evaluate their practicality in luminescent white-light applications. This endeavour was accomplished via rigorous scrutiny of the optical absorption, emission, and colour characteristics.

2. Methods

2.1. Glass preparation

FP glasses doped with Dy³⁺ ions at different concentrations were prepared via melt quenching in the present study. Chemicals such as HIMEDIA NH₄H₂PO₄ (99%) and KF (99.50%), in conjunction with Otto's BiF₃ (99.9%), HIMEDIA MgO (98%), HIMEDIA ZnO (99%), and HIMEDIA Dy₂O₃ (99.99%), were employed in accordance with the empirical formula (60 – *x*) P₂O₅ + 10MgO + 10ZnO + 10BiF₃ + 10KF + *x*Dy₂O₃, with *x* values of 0.1, 0.5, 1.0, 1.5 and 2.0 mol%, respectively. The components of the glass system and their respective codes are detailed in table 1, in a thorough explanation.

The chemicals were mixed in a stoichiometric manner, ground in an agate mortar to promote homogeneity, and packed in aluminium crucibles. The mixture was heated for 1 h at 1150 °C in a programmable electric heating chamber (Indfurr). After quenching a heavy brass plate, the molten substance was forced through another plate. The transparent glasses were annealed at 450 °C for three hours in another electric heating chamber to reduce internal stress. After annealing, the glass was cooled to room temperature.

2.2. Characterization

The refractive indices of the Dy³⁺ ion-doped FP glasses were determined at room temperature using an Abbe ATAGO refractometer operating at a yellow sodium D spectral line of 589 nm, with 1-bromonaphthalene liquid as the contact liquid. The accuracy of this assessment is ±0.001. The density of the Dy³⁺ ion-doped FP glasses was measured at room temperature using a Shimadzu digital weighing balance and Archimedes principle, with deionised water as the immersion liquid. The synthesised Dy³⁺-ion-doped FP glasses were characterised for their amorphousness using a Rigaku Mini Flex 600 x-ray diffractometer with Cuα radiation. Scanning electron microscope (SEM) images were captured using a JSM-IT 500 MODEL manufactured by JEOL, which was fitted with a remarkable AMETEK EDS Device. Using the KBr pellet technique, Fourier transform infrared (FTIR) spectra were collected in the 1500–400 cm⁻¹ range using a Bruker Alpha Compact FTIR spectrophotometer. Raman spectra were acquired using an Invia Reflex Laser Confocal Raman Microscope with Spectrometer (Renishaw Metrological Systems UK) in the range from 100 cm⁻¹ to 1500 cm⁻¹. The optical absorption

Table 1. Glass composition of FP glasses doped with different concentration of Dy³⁺ ions.

Glass system	Composition (mol%)					
	P ₂ O ₅	MgO	ZnO	BiF ₃	KF	Dy ₂ O ₃
FP01Dy	59.9	10	10	10	10	0.1
FP05Dy	59.5	10	10	10	10	0.5
FP10Dy	59.0	10	10	10	10	1.0
FP15Dy	58.5	10	10	10	10	1.5
FP20Dy	58.0	10	10	10	10	2.0

spectra in the UV–Vis–NIR region were recorded at room temperature using a JASCO V570 spectrophotometer with a resolution of 1.0 nm. A JOBIN YVON Fluorolog-3 fluorometer was used to measure the excitation and emission spectra of FP glasses doped with Dy³⁺ ions in the visible region. The instrument was equipped with a double-beam monochromator in front-surface mode (22.5°) and a 450 W-xenon lamp as the measured excitation source.

3. Results and discussion

3.1. Physical properties

At normal temperature, the refractive indices (n) of FP glasses doped with Dy³⁺ were evaluated at concentrations of 0.1, 0.5, 1.0, 1.5, and 2.0 mol%, with values of 1.652, 1.653, 1.653, 1.654, and 1.652, respectively. Correspondingly, the density (ρ) values exhibited a positive linear relationship with the quantity of dysprosium. In particular, the density (ρ) values of Dy³⁺ ions at 0.1, 0.5, 1.0, 1.5, and 2.0 mol% were 2.977, 3.338, 3.855, 4.001, and 4.262, respectively. The density (ρ) was increased with the increment of Dy³⁺ ion concentration whereas the molar volume was decreased from 61.39 (cm³ mol⁻¹) to 43.52 (cm³ mol⁻¹). The increment in density (ρ) may be due to the replacement of lower molecular weight component P₂O₅ (141.944 gm mol⁻¹) with higher molecular weight component Dy₂O₃ (372.998 gm mol⁻¹) [16]. The decrease in the molar volume (V_m) of glass samples due to Dy³⁺ doping can be attributed to decrease in interatomic distance [17]. The increase in density (ρ) and decrease in molar volume (V_m) indicate that the compactness of the prepared FP glasses has increased w.r.to increase the concentration of Dy³⁺ ions [18]. As the concentration of Dy³⁺ ions increase, the interatomic distance between the bonds inside the glass network decreases, resulting in a more compact and dense glass for the prepared glasses. Other physical parameters were calculated using the density (ρ) and refractive index (n) using equations explained elsewhere [19]. The results are presented in table 2.

3.2. X-ray diffraction (XRD) analysis

The powder XRD patterns in figure 1 show the characteristics of FP glasses infused with Dy³⁺ ions. Upon examination, no peaks were detected, suggesting the presence of crystals.

Rather, a broad hump was observed in the 10–40° range, indicative of a lack of crystallisation. Consequently, the XRD profile indicated that the amorphous character of the studied glass samples was preserved.

3.3. Morphological studies

Figure 2(a) presents a surface morphological image obtained through scanning electron microscopy (SEM) of a selected sample of FP20Dy glass. The image offers a clear representation of the smoothness of the glass surface and the absence of crystals. Figure 2(b) shows the EDS spectrum of a typical FP20Dy glass sample. The EDS spectrum depicted in figure 2(b) indicates the presence of components utilised in the manufacturing process of the glass sample being examined.

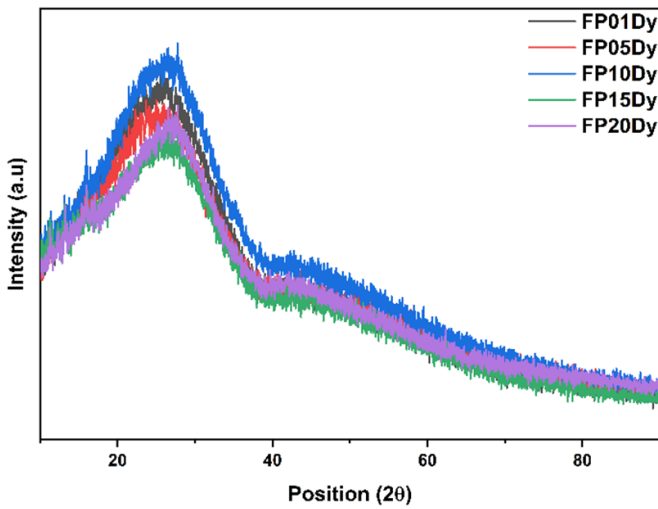
3.4. Vibrational studies (FTIR & Raman spectra)

The mid-infrared range FTIR spectra of FP glasses doped with Dy³⁺ ions were assessed and are shown in figure 3. In the spectra produced by all FP glass samples, four individual IR bands were observed and are labelled (a), (b), (c), and (d). Band (a), observed between 739 and 743 cm⁻¹, is attributed to the symmetric stretching of $\nu_{sy}(P-O-P)$ [7], whereas band (b), observed between 905 and 909 cm⁻¹, denotes the symmetric stretching of the $\nu_{sy}(P-O-P)$ molecule with a linear metaphosphate chain and P–F groups [17]. The symmetric stretching of $\nu_{sy}(PO_4^{3-})$ units generates band (c) between 987 and 1043 cm⁻¹ [21], and band (d) between 1100 and 1102 cm⁻¹ is produced by the same process [4].

Figure 4 shows the deconvoluted Raman spectrum of the glass sample FP20Dy. The Raman bands detected at 343, 524, 696, 1161, and 1234 cm⁻¹ correspond to five distinctive Raman peaks. Notably, the Raman band at 1161 cm⁻¹ exhibited the highest intensity among the five bands. The Raman band at 1161 cm⁻¹ was caused by the symmetric stretching vibration of the O–P–O groups in metaphosphate glass Q¹ tetrahedra [2]. The Raman spectral peak demonstrates the presence of P–F related modes at a wavenumber of 343 cm⁻¹, confirming the existence of skeletal deformation vibrations associated with various phosphate chains and PO₃ deformation [2, 22]. The small Raman peak at 524 cm⁻¹ is associated with the twisting vibrations of the O–P–O and PO₂ modes [17]. The vibrational mode detected at 696 cm⁻¹ was assigned to P–F bonding in the FPO₃²⁻ compound [3]. The Raman spectral feature located at a wavenumber of 1234 cm⁻¹

Table 2. Important physical and optical properties of prepared FP glasses doped with Dy³⁺ ions.

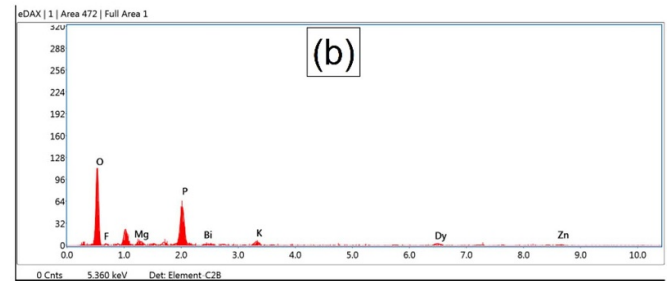
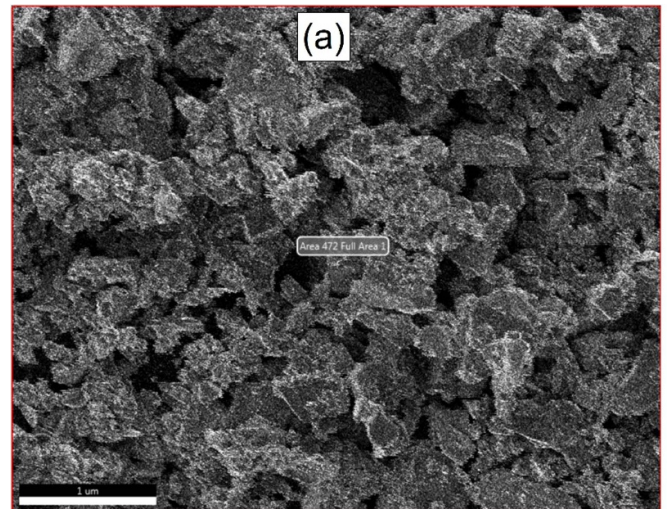
Property	FP01Dy	FP05Dy	FP10Dy	FP15Dy	FP20Dy	BSLNAD5 [20]	STAMB1 [14]
Refractive index (n)	1.652	1.653	1.653	1.654	1.652	2.33	2.254
Thickness t (cm)	0.272	0.284	0.286	0.280	0.275	—	—
Density (gm cm ⁻³)	2.977	3.338	3.855	4.001	4.262	2.716	2.837
Molecular weight M.W (gm mol ⁻¹)	182.75	183.32	184.03	184.75	185.46	—	—
Ion concentration ($N \times 10^{20}$ ion cm ⁻³)	0.098	0.548	1.261	1.956	2.767	48.9	1.164
Molar volume V_m (cm ³ mol ⁻¹)	61.39	54.92	47.74	46.18	43.52	24.62	31.040
Molar refraction R_m (cm ⁻³)	22.45	20.10	17.48	16.92	15.91	14.67	17.889
Inter atomic distance ($\text{Å} \times 10^{20}$)	2.168	1.222	0.926	0.800	0.712	2.37	4.412

**Figure 1.** XRD profiles of FP glasses doped with different concentrations of Dy³⁺ ions.

is indicative of asymmetrical stretching oscillations exhibited by the PO₃ groups [23]. In conclusion, The FTIR spectra of the FP glasses indicated vibrational bands that matched the distinctive phosphate groups, which was further confirmed by Raman analysis.

3.5. Analysis of optical absorption spectra

The optical absorption spectra of the Dy³⁺ ion-doped FP glasses were observed in the UV-V-NIR spectral range, as shown in figure 5. Thirteen peaks were found, seven of which were in the UV-visible range and six of which were in the NIR range. These peaks corresponded to transitions from the ground state ⁶H_{15/2} to ⁴(⁴F,⁴D)_{5/2}, ⁴(⁴M,⁴D)_{15/2}, ⁴I_{11/2}, ⁴I_{13/2} + ⁴F_{7/2}, ⁴G_{11/2}, ⁴I_{15/2}, ⁴F_{9/2}, ⁶F_{3/2}, ⁶F_{5/2}, ⁶H_{5/2} + ⁶F_{7/2}, ⁶H_{7/2} + ⁶F_{9/2}, ⁶H_{9/2} + ⁶F_{11/2}, and ⁶H_{11/2}, respectively, at wavelengths of ~340, ~346, ~361, ~384, ~423, ~449, ~470, ~753, ~802, ~894, ~1086, ~1271, and ~1685 nm. The ⁶H_{15/2} → ⁶H_{9/2} + ⁶F_{11/2} transition occurring at approximately 1271 nm exhibits a greater intensity than the other peaks and is therefore referred to as the hypersensitive transition (HST) [24]. This transition adheres to the selection criteria of $2 \geq |\Delta L|$, $\Delta S = 0$, and $2 \geq |\Delta J|$ [25].

**Figure 2.** (a) SEM image (b) EDS spectra of representative FP20Dy glass sample.

Utilization of the electronic structure obtained through optical absorption is a prevalent technique for the determination of various parameters, including optical energy ($E_{\text{Optical}}^{\text{direct}}$, $E_{\text{Optical}}^{\text{indirect}}$), Urbach energy (ΔU), Nephelauxetic ratio (β), and bonding parameter (δ) [26]. Table 3 displays the absorption peak positions (in cm⁻¹) of Dy³⁺ ions in aqueous solutions and FP glasses, as well as their positions along the 2DyBBCZFB [27], ZBASDy0.5 [28] glass matrices from previous research in the literature. Due to the nephelauxetic effect, Dy³⁺ ions exhibited significant shifts in band positions compared to the aqueous solution [29]. This effect is quantified by parameters β and δ , where β is defined as ν_c/ν_{aqua} . Here, ν_c and ν_{aqua} represent the absorption peak positions (in cm⁻¹) of Dy³⁺ ions in FP glass and aqueous solution, respectively.

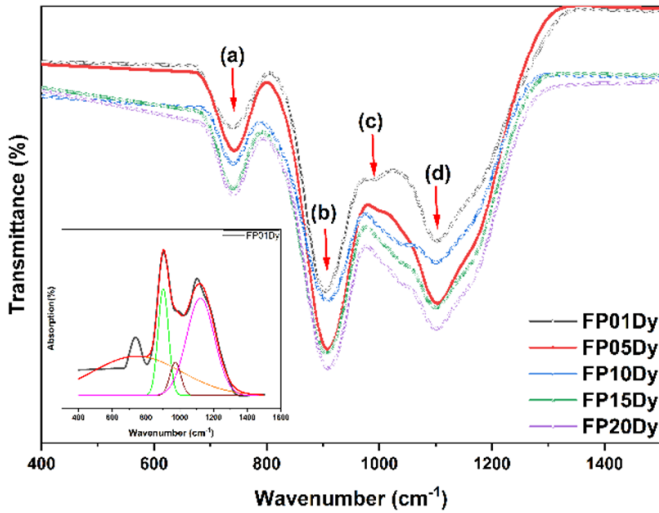


Figure 3. Mid FTIR spectra of FP glasses doped with different concentrations of Dy^{3+} ions in the range $400\text{--}1500\text{ cm}^{-1}$.

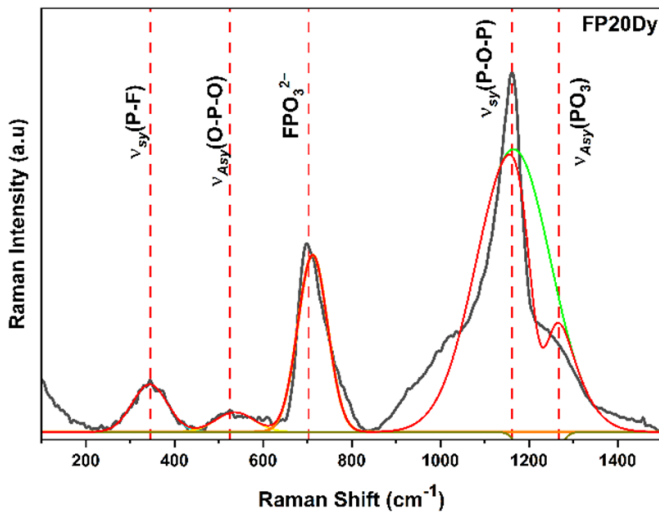


Figure 4. Raman spectrum of FP glass doped with 2.0 mol% of Dy^{3+} ions (deconvoluted).

A minor decrease in the average nephelauxetic value was observed with increasing Dy^{3+} ion concentration. The determination of the bonding parameter (δ) is crucial for understanding the coordination of the RE ion and the ligand bonds surrounding it [30]. The value of δ was determined using the formula obtained from the literature [26] and the results were presented in table 3. The nature of the bonding between Dy^{3+} ions and their neighbouring host can be either ionic or covalent, depending on the presence of a positive or negative value for δ , respectively [31]. The negative value of δ suggests the ionic bonding nature of the Dy-ligand bond.

The optical energy ($E_{\text{Optical}}^{\text{direct}}$, $E_{\text{Optical}}^{\text{indirect}}$), encompassing both the direct and indirect values, along with the Urbach energy, represented by the symbol ΔU , are critical parameters for amorphous materials [32]. The plotting of Tauc plots, in accordance with Davis and Mott’s law [33], was utilised for direct allowed and indirect allowed transitions, as shown in

figure 6. By examining the plotted Tauc plots, both the direct and indirect bandgap energies were determined and are listed in table 4. Up to 1.5 mol%, the optical energy ($E_{\text{Optical}}^{\text{direct}}$, $E_{\text{Optical}}^{\text{indirect}}$) decreases as the concentration of Dy_2O_3 increases; after that, it shows an increasing trend. The energy of the direct bandgap, signified as $E_{\text{Optical}}^{\text{direct}}$, undergoes a decline from 3.78 eV (0.1 mol%) to 3.69 eV (1.5 mol%) and then an increase to 3.72 eV (2.0 mol%). In parallel, the energy of the indirect bandgap, referred to as $E_{\text{Optical}}^{\text{indirect}}$, undergoes a decrease from 3.37 eV (0.1 mol%) to 3.27 eV (1.5 mol%) and subsequently increases to 3.34 eV (2.0 mol%). The alteration in the $E_{\text{Optical}}^{\text{direct}}$, and $E_{\text{Optical}}^{\text{indirect}}$ values as a function of concentration can be explicated from the perspective of the modification in structure. The Urbach energy, commonly referred to as ΔU , is an optical property that provides insight into the level of disorder in glass samples [18]. The ΔU value increase from 0.27 eV (0.1 mol%) to 0.32 eV (1.5 mol%) before subsequently decreasing with the progressive addition of Dy^{3+} ions. These findings suggest that the disorder within the glass material experiences a rise in correlation with the presence of Dy^{3+} ions, up to a concentration of 1.5 mol%. However, beyond this threshold, a decrease in disorder was observed in the glass samples.

3.6. Analysis of Judd–Ofelt (JO) intensity parameters

JO theory has been applied to calculate theoretical (f_{cal}) and experimental (f_{exp}) oscillator strengths for the different transitions found in the absorption spectra of Dy^{3+} ion-containing FP glasses. Oscillator strength is a dimensionless quantity that measures the probability of transitions to occur between the energy levels in the atoms or molecules [36]. The root mean square deviation (δ_{RMS}) describes the quality of the fit between the experimental (f_{exp}) and theoretical (f_{cal}) oscillator strength of the experiment [37]. The small values of the root mean square deviation emphasize a good quality of fit between f_{exp} and f_{cal} [38]. The calculations were based on the equations established in previous studies [26], and the root mean square deviation magnitudes (δ_{RMS}) were also determined. Table 5 presents the results of the analysis. An examination of table 5 reveals that the transition from ${}^6H_{15/2}$ to ${}^6H_{9/2} + {}^6F_{11/2}$, which occurs at approximately 1271 nm, displays significant oscillator strengths (f_{exp} , f_{cal}). It can be observed that the oscillator strengths (f_{exp} and f_{cal}) of FP01Dy glass showed a higher value when compared to the studied FP glasses including the ZBASDy0.5 [28], BTPZNAL 0.1D [31] glasses doped with Dy^{3+} ions. Greater radiative transition probabilities are indicated by stronger oscillator strengths, which in turn result in stronger fluorescence emission intensities [39]. This observation suggests that the FP01Dy may have stronger fluorescence emission intensities. Moreover, the δ_{RMS} values for the FP glasses doped with Dy^{3+} ions were quite low (3.04, 2.22, 1.97, 0.74, and 0.62), indicating a strong fit between the experimental and theoretical oscillator strengths, and confirming the accuracy of the JO intensity parameters.

Two well-known scientists with the name B R Judd, and G S Ofelt, A theory known as the JO theory was put forth in the 1960s and it describes the intensities of actinide and lanthanide

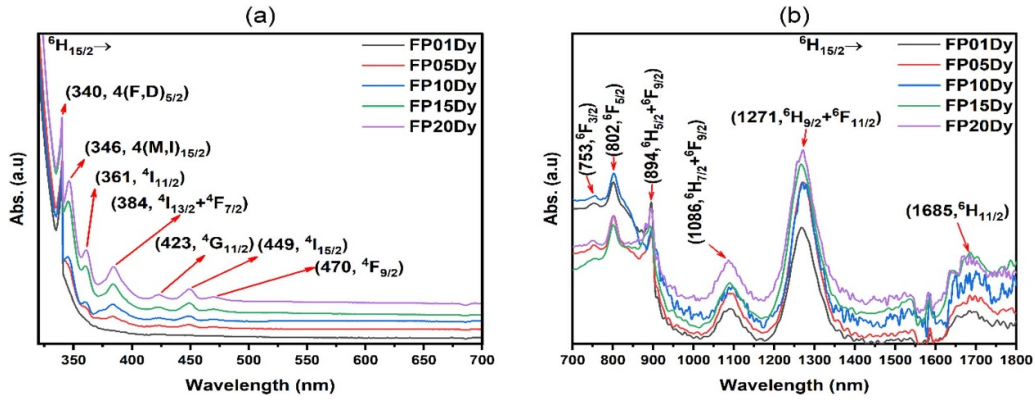


Figure 5. Optical absorption spectra of FP glasses doped with different concentrations of Dy³⁺ ions (a) UV–Visible range (b) NIR range.

Table 3. Absorption peak positions (in cm⁻¹) of FP glasses (ν_c) and aqueous solution (ν_{aqua}), nephelauxetic ratios ($\bar{\beta}$), and bonding parameters (δ) of glasses doped with Dy³⁺ ions.

	FP01Dy	FP05Dy	FP10Dy	FP15Dy	FP20Dy	2Dy BBCZFB [27]	ZBASDy0.5 [28]	ν_{aqua}
Energy level ${}^6\text{H}_{15/2} \rightarrow$	ν_c	ν_c	ν_c	ν_c	ν_c	ν_c	ν_c	
${}^6\text{H}_{11/2}$	5942	5935	5882	5935	5935	5983	5920	5833
${}^6\text{H}_{9/2} + {}^6\text{F}_{11/2}$	7886	7868	7874	7893	7868	7904	7898	7700
${}^6\text{H}_{7/2} + {}^6\text{F}_{9/2}$	9191	9191	9124	9191	9200	9221	9233	9100
${}^6\text{H}_{5/2} + {}^6\text{F}_{7/2}$	11 173	11 173	11 161	11 211	11 186	11 146	11 185	11 000
${}^6\text{F}_{5/2}$	12 500	12 484	12 453	12 500	12 500	12 534	12 500	12 432
${}^6\text{F}_{3/2}$	13 333	13 316	13 245	13 298	13 351	13 281	13 315	13 212
${}^4\text{F}_{9/2}$	—	—	21 322	21 277	21 322	21 261	21 231	21 100
${}^4\text{I}_{15/2}$	—	22 272	22 272	22 272	22 272	22 160	22 123	22 100
${}^4\text{G}_{11/2}$	—	23 585	23 641	23 641	23 641	23 475	23 474	23 400
${}^4\text{I}_{13/2} + {}^4\text{F}_{7/2}$	—	26 110	26 110	26 042	26 042	25 802	25 906	25 800
${}^4\text{I}_{11/2}$	—	27 855	27 855	27 778	27 701	—	27 472	27 503
$({}^4\text{M}, {}^4\text{D})_{15/2}$	—	28 736	28 736	28 986	28 902	28 343	28 735	29 244
$({}^4\text{F}, {}^4\text{D})_{5/2}$	29 412	29 326	29 412	29 412	29 412	—	—	29 593
$\bar{\beta}$	1.011	1.008	1.006	1.009	1.008	1.0087	1.006 75	
δ	-1.0892	-0.7542	-0.5964	-0.8920	-0.7937	-0.8625	-0.6705	

transitions in solids and solutions [40]. JO theory is used to determine three phenomenological parameters, Ω_λ ($\lambda = 2, 4, 6$) called JO parameters [40]. Among the three parameters, the values of Ω_4 and Ω_6 represent the bulk characteristics of the medium, such as stiffness and viscosity, the Ω_2 value often indicates the degree of asymmetry and covalency between the RE ions and local ligand anions [29]. It is feasible to gain a deeper understanding of the nearby framework encompassing rare-earth ions via an analysis of the JO parameters Ω_λ (where $\lambda = 2, 4, 6$) [41]. The JO parameters Ω_λ (where $\lambda = 2, 4, 6$) of the current-doped Dy³⁺ ion FP glasses were calculated using a formula published in the literature [42]. Table 6 presents the results along with data from previous glasses doped with Dy³⁺ ions. The JO intensity parameter Ω_λ ($\lambda = 2, 4, 6$) values exhibited the same trends for each glass, with $\Omega_6 > \Omega_2 > \Omega_4$. This JO parameter trend has been observed in various Dy³⁺ ion-infused glass systems including Alumino borosilicate Dy_{0.1} [26], BPbAZLNdy_{1.0} [43], BSLZfDy_{1.0} [44], and BSAZNfDy_{1.0} [5]. However, each glass system has

distinct intensity, covalence, and asymmetry factors. JO parameters of FP01Dy glass showed significant higher values when compared with other glasses such as Alumino borosilicate Dy_{0.1} [26], BPbAZLNdy_{1.0} [43], BSLZfDy_{1.0} [44], and BSAZNfDy_{1.0} [5].

This study found that in all FP glasses, the Ω_6 values were higher than the Ω_2 values, indicating high rigidity. The Ω_2 value is significantly affected by the HSTs observed in the absorption spectra, providing insights into the bonding between Dy and O [45]. The JO parameters exhibited variations in relation to the glass composition in the order of FP01Dy > FP05Dy > FP10Dy > FP20Dy > FP15Dy. The JO parameters decreased as the concentration of Dy³⁺ ions from 0.1 to 1.5 mol%. However, upon further increasing the Dy³⁺ concentration, the JO parameters increased. As the concentration of Dy³⁺ ions increase from 0.1 to 1.5 mol%, there is a corresponding decrease in the magnitude of Ω_2 , which suggests a decrease in the covalency of the Dy–O bond [33]. Nevertheless, when the concentration of Dy³⁺ ions exceed

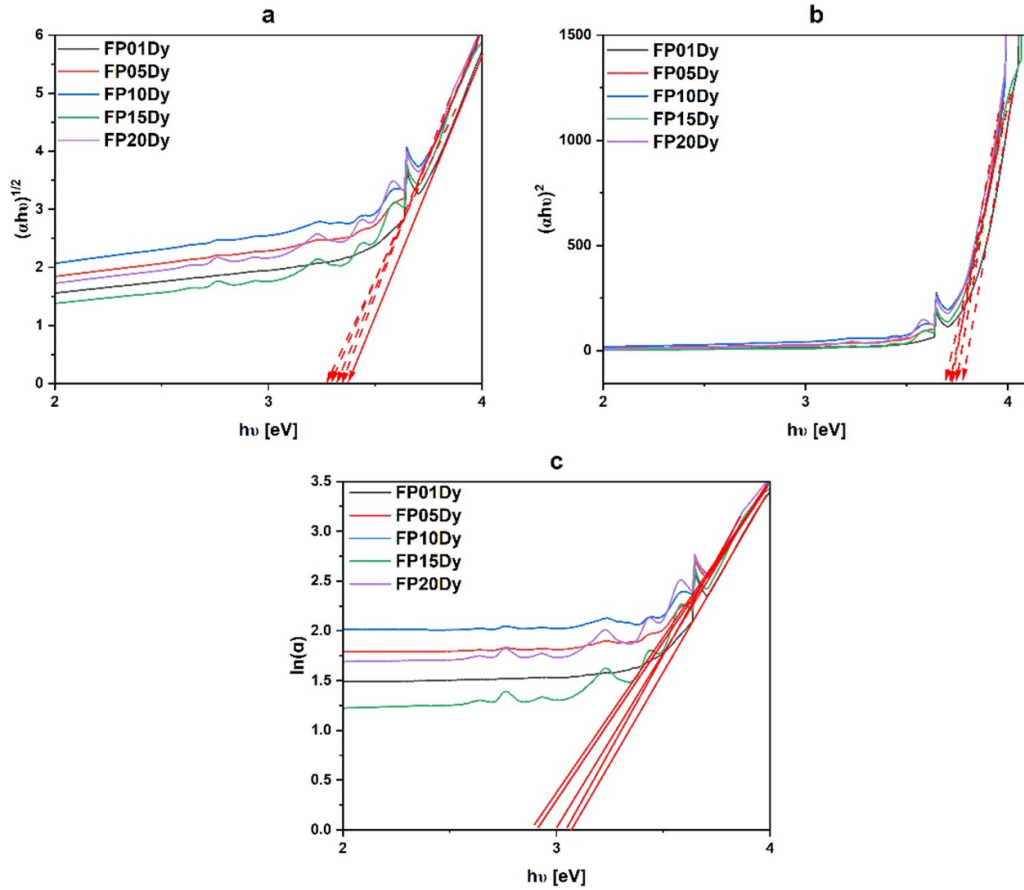


Figure 6. A Tauc’s plot for (a) indirect bandgap (b) Tauc’s plot for direct bandgap and (c) Urbach plot of prepared FP glasses doped with various concentrations of Dy³⁺ ions.

Table 4. Optical energies ($E_{\text{Optical}}^{\text{direct}}$, $E_{\text{Optical}}^{\text{indirect}}$, eV) and Urbach energies (ΔU , eV) of glasses doped with Dy³⁺ ions.

	FP01Dy	FP05Dy	FP10Dy	FP15Dy	FP20Dy	NBZD10 [34]	GP05 [35]	TBZDy05 [33]	0.05DyBBCZFB [27]
$E_{\text{Optical}}^{\text{direct}}$	3.78	3.74	3.71	3.69	3.72	3.27	4.33	3.09	2.994
$E_{\text{Optical}}^{\text{indirect}}$	3.37	3.31	3.29	3.27	3.34	2.56	4.23	3.20	2.831
ΔU	0.27	0.29	0.31	0.32	0.26	0.73	0.20	0.25	0.615

1.5 mol%, the Ω_2 value exhibited a positive correlation, indicating an increase in the covalency of the Dy–O bond as a result of the cross-relaxation phenomenon. The glass FP01Dy exhibits significant JO parameters, specifically Ω_2 (44.14×10^{-20}), Ω_4 (7.98×10^{-20}) and Ω_6 (46.08×10^{-20}), indicating its exceptional quality. Among the various glass systems mentioned, FP01Dy glass exhibits notable levels of stiffness, asymmetry, and covalent bonding between Dy³⁺ and local ligand anions.

3.7. Photoluminescence analysis and radiative properties

Figure 7 presents the excitation spectra of FP15Dy glass, specifically at an emission wavelength of 572 nm. Despite variations in intensity, the remaining glasses exhibited shapes similar to those of the FP15Dy glass. The spectra showed six excitation bands at wavelengths of 323, 348, 363,

387, 425, and 452 nm, corresponding to various transitions, ${}^6\text{H}_{15/2} \rightarrow ({}^4\text{K}_{15/2} + {}^6\text{P}_{3/2})$, ${}^6\text{H}_{15/2} \rightarrow ({}^4\text{M} + {}^4\text{I})_{15/2}$, ${}^6\text{H}_{15/2} \rightarrow {}^4\text{I}_{11/2}$, ${}^6\text{H}_{15/2} \rightarrow ({}^4\text{I}_{13/2} + {}^4\text{F}_{7/2})$, ${}^6\text{H}_{15/2} \rightarrow {}^4\text{G}_{11/2}$, and ${}^6\text{H}_{15/2} \rightarrow {}^4\text{I}_{15/2}$, respectively. Among the several transitions obtained, the transition denoted as ${}^6\text{H}_{15/2} \rightarrow ({}^4\text{I}_{13/2} + {}^4\text{F}_{7/2})$ at a wavelength of 387 nm demonstrated the greatest intensity. Consequently, this particular transition is well suited for monitoring the emission characteristics of the created FP glasses.

Figure 8 shows the emission spectra of Dy³⁺ ion-doped FP glasses excited at 387 nm in the UV–Vis region. The spectra illustrate three notable bands: the blue band (${}^4\text{F}_{9/2} \rightarrow {}^6\text{H}_{15/2}$) at a wavelength of 481 nm, yellow band (${}^4\text{F}_{9/2} \rightarrow {}^6\text{H}_{13/2}$) at a wavelength of 572 nm, and red band (${}^4\text{F}_{9/2} \rightarrow {}^6\text{H}_{11/2}$) at a wavelength of 660 nm [15]. The blue band (${}^4\text{F}_{9/2} \rightarrow {}^6\text{H}_{15/2}$) is ascribed to the magnetic dipole interaction, which is unaffected by the specific crystal field environment [13]. The

Table 5. Experimental, calculated oscillator strengths (f_{exp} & $f_{cal} \times 10^{-6}$) and root mean square deviations ($\delta_{RMS} \times 10^{-6}$) of glasses doped with Dy³⁺ ions.

Energy level ⁶ H _{15/2} →	FP01Dy		FP05Dy		FP10Dy		FP15Dy		FP20Dy		ZBASDy0.5 [28]		BTPZNAL 0.1D [31]	
	f_{exp}	f_{cal}	f_{exp}	f_{cal}	f_{exp}	f_{cal}	f_{exp}	f_{cal}	f_{exp}	f_{cal}	f_{exp}	f_{cal}	f_{exp}	f_{cal}
⁶ H _{11/2}	22.89	20.16	6.60	6.92	3.15	3.21	2.20	2.22	2.72	2.69	0.935	0.821	0.951	1.295
⁶ H _{9/2} + ⁶ F _{11/2}	52.36	52.71	15.13	15.15	8.00	8.04	4.74	4.76	6.16	6.18	2.088	2.104	9.277	9.233
⁶ H _{7/2} + ⁶ F _{9/2}	42.09	36.45	11.44	12.21	6.27	6.79	4.02	4.18	4.86	4.93	0.923	1.538	2.076	2.162
⁶ H _{5/2} + ⁶ F _{7/2}	40.87	38.04	10.17	13.29	4.06	6.52	3.10	4.39	4.11	5.20	2.005	1.571	1.921	1.692
⁶ F _{5/2}	56.67	59.90	13.96	7.05	7.99	3.28	4.36	2.29	4.29	2.73	0.868	0.819	1.688	0.765
⁶ F _{3/2}	29.23	27.75	7.58	7.33	3.24	3.62	2.43	2.43	2.59	2.52	0.430	0.153	0.467	0.144
⁴ F _{9/2}	—	—	—	—	4.53	3.51	2.20	2.34	1.68	1.41	0.871	0.121	0.320	0.129
⁴ I _{15/2}	—	—	12.24	12.58	5.64	1.19	3.31	3.83	2.67	2.00	0.981	0.301	0.674	0.426
⁴ G _{11/2}	—	—	18.29	18.07	7.55	7.11	2.71	2.04	2.82	2.14	1.003	0.016	0.356	0.076
⁴ I _{13/2} + ⁴ F _{7/2}	—	—	29.14	29.61	22.29	21.65	9.47	9.92	6.83	6.28	1.700	0.205	—	—
⁴ I _{11/2}	—	—	11.48	11.34	6.07	6.16	4.21	4.11	3.35	3.13	1.654	0.359	—	—
(⁴ M, ⁴ D) _{15/2}	—	—	21.71	21.12	11.73	11.06	7.14	7.04	5.33	5.15	2.205	0.687	—	—
(⁴ F, ⁴ D) _{5/2}	17.53	15.38	14.13	14.19	6.76	6.56	4.72	4.39	2.61	2.46	—	—	—	—
δ_{RMS}	±3.04		±2.22		±1.97		±0.74		±0.62		±0.862		±0.371	

Table 6. Judd–Ofelt (JO) intensity parameters ($\Omega_2, \Omega_4, \Omega_6 \times 10^{-20} \text{ cm}^2$) and their trend in different FP glasses doped with Dy³⁺ ions.

Glass system	Judd–Ofelt intensity parameters			Trend
	Ω_2	Ω_4	Ω_6	
FP01Dy [Present Work]	44.14	7.98	46.08	$\Omega_6 > \Omega_2 > \Omega_4$
FP05Dy [Present Work]	12.15	1.48	16.35	$\Omega_6 > \Omega_2 > \Omega_4$
FP10Dy [Present Work]	05.02	2.85	07.62	$\Omega_6 > \Omega_2 > \Omega_4$
FP15Dy [Present Work]	03.35	0.88	05.30	$\Omega_6 > \Omega_2 > \Omega_4$
FP20Dy [Present Work]	04.80	0.94	06.33	$\Omega_6 > \Omega_2 > \Omega_4$
Alumino borosilicate Dy _{0.1} [26]	12.59	0.45	17.52	$\Omega_6 > \Omega_2 > \Omega_4$
BPbAZLNdy _{1.0} [43]	03.85	3.12	08.00	$\Omega_6 > \Omega_2 > \Omega_4$
BSLZfDy _{1.0} [44]	02.42	0.80	02.65	$\Omega_6 > \Omega_2 > \Omega_4$
BSAZNfDy _{1.0} [5]	15.50	0.38	17.70	$\Omega_6 > \Omega_2 > \Omega_4$

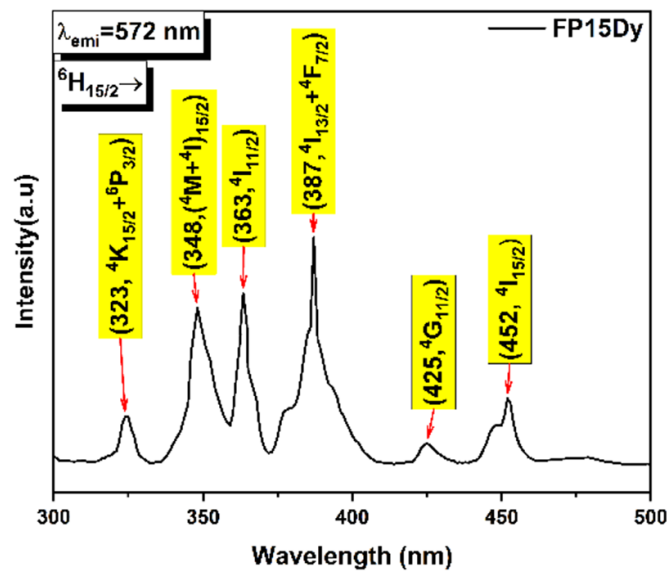


Figure 7. Excitation spectra of representative FP glass doped with 1.5 mol% of Dy³⁺ ions.

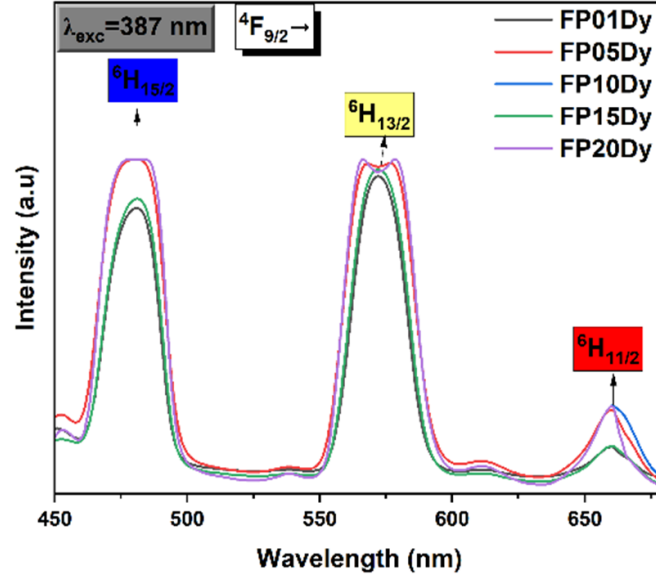


Figure 8. Emission spectra of FP glasses doped with different concentrations of Dy^{3+} ions.

Table 7. Peak wavelength of emissions (λ_p , nm), effective bandwidths ($\Delta\lambda_{\text{eff}}$, nm), branching ratios (β_{exp} , β_{cal} , %), stimulated emission cross-sections ($\sigma_p \times 10^{-21}$ cm²), and gain bandwidths ($(\Delta\lambda_{\text{eff}} \times \sigma_p) \times 10^{-25}$ cm³) of ${}^4\text{F}_{9/2} \rightarrow {}^6\text{H}_{15/2}$, ${}^4\text{F}_{9/2} \rightarrow {}^6\text{H}_{13/2}$ and ${}^4\text{F}_{9/2} \rightarrow {}^6\text{H}_{11/2}$ transitions of present FP glasses doped with Dy^{3+} ions.

	λ_p	A_R	$\Delta\lambda_{\text{eff}}$	β_{exp}	β_{cal}	σ_p	$\Delta\lambda_{\text{eff}} \times \sigma_p$
FP01Dy							
${}^4\text{F}_{9/2} \rightarrow {}^6\text{H}_{15/2}$	481	2430.8	13.88	40.93	0.296	03.79	052.65
${}^4\text{F}_{9/2} \rightarrow {}^6\text{H}_{13/2}$	572	4905.0	16.25	55.02	0.598	12.66	205.69
${}^4\text{F}_{9/2} \rightarrow {}^6\text{H}_{11/2}$	662	0377.1	37.03	04.05	0.046	2.97	110.03
FP05Dy							
${}^4\text{F}_{9/2} \rightarrow {}^6\text{H}_{15/2}$	481	0846.6	11.20	41.08	0.321	01.07	011.95
${}^4\text{F}_{9/2} \rightarrow {}^6\text{H}_{13/2}$	576	1531.4	12.59	51.98	0.580	03.12	039.32
${}^4\text{F}_{9/2} \rightarrow {}^6\text{H}_{11/2}$	661	0110.1	31.77	06.93	0.042	00.74	023.61
FP10Dy							
${}^4\text{F}_{9/2} \rightarrow {}^6\text{H}_{15/2}$	480	0421.5	10.13	42.91	0.324	00.48	004.84
${}^4\text{F}_{9/2} \rightarrow {}^6\text{H}_{13/2}$	572	0738.0	12.28	51.22	0.568	01.47	018.08
${}^4\text{F}_{9/2} \rightarrow {}^6\text{H}_{11/2}$	661	0052.2	27.92	05.88	0.040	00.31	008.64
FP15Dy							
${}^4\text{F}_{9/2} \rightarrow {}^6\text{H}_{15/2}$	481	0284.7	13.14	41.45	0.332	00.42	005.52
${}^4\text{F}_{9/2} \rightarrow {}^6\text{H}_{13/2}$	572	0488.2	15.67	53.97	0.568	01.22	019.05
${}^4\text{F}_{9/2} \rightarrow {}^6\text{H}_{11/2}$	660	0033.7	32.37	04.57	0.039	00.23	007.47
FP20Dy							
${}^4\text{F}_{9/2} \rightarrow {}^6\text{H}_{15/2}$	481	0332.7	13.67	40.24	0.318	00.51	006.99
${}^4\text{F}_{9/2} \rightarrow {}^6\text{H}_{13/2}$	572	0608.0	16.45	54.12	0.581	01.59	026.16
${}^4\text{F}_{9/2} \rightarrow {}^6\text{H}_{11/2}$	660	0044.0	28.46	5.63	0.042	00.27	007.55

yellow band, namely, the transition from ${}^4\text{F}_{9/2}$ to ${}^6\text{H}_{13/2}$, can be attributed to an induced electric dipole (ED) interaction [14]. The ED transition band at 572 nm has the highest intensity among the two transition bands and is referred to as the HST, which obeys the selection rule ($\Delta J = 0 \pm 2$) [22].

The radiative properties of the prepared FP glasses containing Dy^{3+} ions were estimated by employing the JO parameters and refractive indices, enabling the analysis of various emission spectra [19]. The results are presented in table 7. As demonstrated in table 7, the yellow band (${}^4\text{F}_{9/2} \rightarrow {}^6\text{H}_{13/2}$) displays a substantial radiative

transition probability (A_R), effective bandwidth ($\Delta\lambda_{\text{eff}}$, nm), experimental branching ratio (β_{exp} , %), stimulated emission cross-section ($\sigma_p \times 10^{-21}$ cm²), and gain bandwidth ($(\Delta\lambda_{\text{eff}} \times \sigma_p) \times 10^{-25}$ cm³) among the three transitional bands. The analysis of laser characteristics requires consideration of the stimulated emission cross-section (σ_p), which is a crucial parameter in the area of laser physics and optical engineering [46]. The Füchtbauer–Ladenburg equation was used to calculate the stimulated emission cross-section (σ_p) [47]. Upon increasing the concentration of Dy^{3+} ions, the stimulated emission cross-section (σ_p) values decreased by up

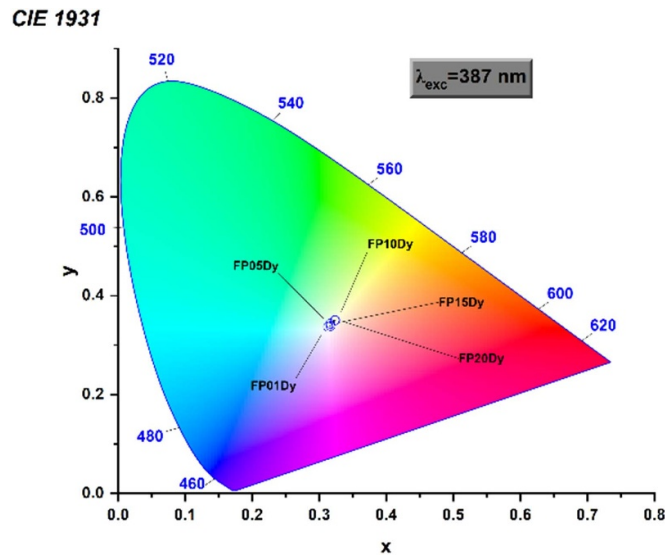


Figure 9. Colour coordinates of FP glasses doped with different concentrations of Dy³⁺ ions excited at a wavelength of 387 nm in the 1931 CIE colour chart.

Table 8. CIE 1931 chromaticity colour coordinates (x_c, y_c), correlated colour temperatures (CCT, K) and yellow to blue luminescence ratios (Y/B) of prepared glass samples.

Glass system	Chromaticity coordinates		CCT	Y/B ratio
	x_c	y_c	Kelvin K	
FP01Dy [Present work]	0.313	0.337	6437	1.34
FP05Dy [Present work]	0.317	0.339	6231	1.27
FP10Dy [Present work]	0.324	0.350	5864	1.19
FP15Dy [Present work]	0.316	0.343	6242	1.30
FP20Dy [Present work]	0.323	0.350	5894	1.34
YAG + Blue Chips [51]	0.29	0.30	5610	—
Standard D50 White light illuminate [51]	0.333	0.333	5455	—
Standard D65 White light illuminate [51]	0.310	0.340	6504	—

to 1.5 mol%. However, beyond this point, the stimulated emission cross-section (σ_p) values exhibit an increase. Among the fabricated FP glasses, the FP01Dy glass had elevated values of A_R , $\Delta\lambda_{eff}$, (β_{exp} , and β_{cal}), σ_p , and ($\Delta\lambda_{eff} \times \sigma_p$) compared to the others. The Y/B ratio, which signifies the relative intensity of the yellow band to the blue band, is an important metric for glasses doped with Dy³⁺ ions [5, 33]. By manipulating the Y/B ratio, it is feasible to attain a specific white-light emission [48, 49]. The values of the Y/B ratios are listed in table 8. It is noteworthy that the acquired Y/B ratios were greater than 1 (>1), which is indicative of the elevated covalency of Dy³⁺ ions [28, 50]. This outcome mirrors that of the JO intensity parameters listed in table 6. Based on the results obtained, it can be inferred that FP01Dy glass is a suitable contender for visible-laser applications.

3.8. Analysis of emission colour

Dy³⁺ ion-doped FP glasses were excited at a wavelength of 387 nm, and the emission spectra were subsequently utilised to establish colour coordinates [8]. The acquired colour

coordinates are depicted in the 1931 CIE colour chart, as illustrated in figure 9. Table 8 presents the results. These colour coordinates can be found within the white region and are situated in close proximity to the neutral point [28] and standard white light illuminate D65 [51]. Utilising the McCamy’s approximation methodology [52], the correlated colour temperature (CCT) was calculated, and the results are shown in table 8.

The determined CCT values fell within the range of 5864–6437 K. The obtained CCT values are close proximity to the CCT of standard white light illuminate D65 [51]. It can be observed that the CCT values of FP glasses doped with Dy³⁺ ions showed a higher value compared to YAG + Blue chip [51], and standard white illuminate D50 [51]. The observed CCT values indicates that the prepared Dy³⁺ ions doped FP glasses are capable of generation of cool white light (5000 K and above). Among the several FP glasses that were fabricated, it was observed that the FP01Dy glass displayed a significantly elevated CCT value of 6437 K. This finding suggests that FP01Dy glass is good candidate for white light generation.

4. Conclusion

Different concentrations of Dy³⁺ ion-doped FP glasses with compositions of (60 - x) P₂O₅ + 10MgO + 10ZnO + 10BiF₃ + 10KF + xDy₂O₃, where x = (0.1, 0.5, 1.0, 1.5, and 2.0), were prepared using the melt-quenching technique. The amorphous nature of the FP glasses was confirmed by SEM and examination of their XRD patterns. Furthermore, the presence of elements in the composition was confirmed using EDX. The FTIR spectra of the FP glasses indicated vibrational bands that matched the distinctive phosphate groups, which was further confirmed by Raman analysis. The bonding parameter (δ) values derived in this investigation were negative, signifying the establishment of ionic bonds between the Dy³⁺ ions and ligands present in all glass matrices. The introduction of Dy₂O₃ resulted in a reduction in both the direct and indirect optical band gaps up to a concentration of 1.5 mol%. Beyond this concentration, the trend exhibited an upward trajectory. Conversely, the inclusion of Dy³⁺ ions resulted in an increase in Urbach Energy up to a concentration of 1.5 mol%, followed by reduction with the addition of Dy³⁺ ions. The elevation in the Urbach energy was strongly correlated with the growth in the irregularity of the sample.

The application of the JO theory enabled the experimental evaluation of the optical absorption spectra, followed by the calculation of the intensity parameters. Dy³⁺ ion-doped FP glasses exhibited a consistent trend, where Ω_6 was greater than Ω_2 and Ω_4 , as demonstrated by the JO intensity parameters. The excitation spectra at an emission wavelength of $\lambda_{\text{emi}} = 572$ nm revealed six excitation bands, and at an excitation wavelength of $\lambda_{\text{exc}} = 387$ nm, three bands were attributed to the emission transition ${}^4F_{9/2} \rightarrow {}^6H_P$ ($P = 15/2, 13/2, 11/2$). Of the three emission transitions, the ${}^4F_{9/2} \rightarrow {}^6H_{13/2}$ transition emitted yellow light at a wavelength of 572 nm. The Y/B ratio for the intensity values was higher than 1, indicating considerable covalency of the Dy³⁺ ions. Among the prepared FP glasses doped with Dy³⁺ ions, FP01Dy glass exhibited high A_R , $\Delta\lambda_{\text{eff}}$, σ_P , and $\Delta\lambda_{\text{eff}} \times \sigma_P$ values, suggesting its potential as a viable option for visible-laser applications. The CIE colour coordinates (x, y) and CCT obtained were located within the white region, with FP01Dy glass demonstrating a high CCT value of 6437 K, confirming the suitability of FP glasses doped with varying concentrations of Dy³⁺ ions for white-light applications.

Data availability statement

All data that support the findings of this study are included within the article (and any supplementary files).

Acknowledgment

The authors thank Mr Essaki Kumar, a laboratory technician at CIF Pondicherry University who helped obtain excitation, emission, and Raman data; the Faculty of Physics and Chemistry at Yogi Vemana University for facilitating the instrumentation of XRD, SEM-EDS, and FTIR; and the

Faculty of Physics at Sri Venkateshwara University for facilitating the instrumentation of the UV-VIS-NIR spectrometer.

Author contributions

K V R: Conceptualization, Writing-Original draft preparation, Investigation, Writing-Review & Editing, Supervision
S V S: Conceptualization, Methodology, Validation, Investigation, Visualization, S J D: Conceptualization, Investigation, Writing-Review & Editing, Visualization, N V S: Conceptualization, Investigation, Writing-Review & Editing, Visualization.

Funding

No funding source to disclose.

Conflict of interest

The authors declare that they have no relevant financial or non-financial interests to disclose.

ORCID iD

K Venkata Rao  <https://orcid.org/0000-0001-5749-3158>

References

- [1] Meejitpaisan P, Kaewjaeng S, Ruangthawee Y, Sangwarantee N and Kaewkhao J 2021 *Mater. Today: Proc.* **43** 2574–87
- [2] Sreedhar V B, Venkata Krishnaiah K, Nayab Rasool S K, Venkatramu V and Jayasankar C K 2019 *J. Non-Cryst. Solids* **505** 115–21
- [3] Möncke D and Eckert H 2019 *J. Non-Cryst. Solids X* **3** 100026
- [4] Rajagukguk J, Sarumaha C S, Chanthima N, Wantana N, Kothan S, Wongdamern N and Kaewkhao J 2021 *Radiat. Phys. Chem.* **185** 109520
- [5] Chandrappa V, Basavapoornima C, Kesavulu C R, Babu A M, Depuru S R and Jayasankar C K 2022 *J. Non-Cryst. Solids* **583** 121466
- [6] Shwetha M and Eraiah B 2021 *J. Non-Cryst. Solids* **555** 120622
- [7] Rao C N, Rao P V, Kameswari R, Raju R R, Chandana G, Samatha K, Srinivas Prasad M V V K, Venkateswarlu M, Naveen A and Dhar G G 2021 *J. Mol. Struct.* **1243** 130784
- [8] Zaman F, Srisittipokakun N, Rooh G, Khattak S A, Kaewkhao J, Rani M and Kim H J 2021 *Opt. Mater.* **119** 111308
- [9] Siva Raju D, Deva Prasad Raju B, Hima Bindu S, Hema Latha M, Suresh Krishna J, Vinay Krishna V and Linga Raju C 2021 *Mater. Today: Proc.* **47** 4364–72
- [10] Elisa M et al 2021 *J. Non-Cryst. Solids* **556** 120569
- [11] Rasool S N, Naveen Kumar K, Lingaswamy A P, Shabeena S, Kesavulu C R and Babu S 2023 *J. Mater. Sci.: Mater. Electron.* **34** 1695
- [12] Kashif I and Ratep A 2023 *Results Opt.* **11** 100401
- [13] Kuwik M, Górný A, Pisarski W A and Pisarska J 2022 *Spectrochim. Acta A* **268** 120693
- [14] Abdullahi I, Hashim S, Sayyed M I and Ghoshal S K 2023 *Heliyon* **9** e15906

- [15] Bairagi S, Bartwal K S and Ansari G F 2023 *Mater. Today Proc.* **80** 799–805
- [16] Kiwsakunkran N, Chanthima N, Kim H J, Kidkhunthod P and Kaewkhao J 2023 *Radiat. Phys. Chem.* **208** 110890
- [17] Ahmadi F, Hussin R and Ghoshal S K 2021 *Optik* **227** 166000
- [18] Mariselvam K and Liu J 2021 *Opt. Mater.* **114** 110997
- [19] Komal Poojha M K, Vijayakumar M, Matheswaran P, Sayed Yousef E and Marimuthu K 2022 *Opt. Laser Technol.* **156** 108585
- [20] Elkhoshkhany N, Marzouk S, El-Sherbiny M, Anwer H, Alqahtani M S, Algarni H, Reben M and Sayed Yousef E 2021 *Results Phys.* **27** 104544
- [21] Ravi Kumar V, Ashirvadam A, Naresh P, Naga Raju G, Ramachandra Rao M V, Kumar Reddy B N and Sahaya Baskaran G 2021 *Opt. Mater.* **121** 111590
- [22] Vidhi A, Anu and Rao A S 2022 *Opt. Mater.* **132** 112863
- [23] Dhavamurthy M, Vinothkumar P, Mohapatra M, Suresh A and Murugasen P 2022 *Spectrochim. Acta A* **266** 120448
- [24] Ravi N, Neelima G, Reddy Nallabala N K, Kummara V K, Ravanamma R, Reddy V J, Prasanth M, Suresh K, Babu P and Venkatramu V 2021 *Opt. Mater.* **111** 110593
- [25] Sailaja P, Mahamuda S, Swapna K, Venkateswarlu M and Rao A S 2021 *Mater. Sci. Eng. B* **270** 115198
- [26] Kashif I and Ratep A 2022 *Bol. Soc. Esp. Ceram. Vidr.* **61** 622–33
- [27] Mariselvam K and Liu J 2021 *Opt. Laser Technol.* **140** 106944
- [28] Monisha M, Mazumder N, Lakshminarayana G, Mandal S and Kamath S D 2021 *Ceram. Int.* **47** 598–610
- [29] Liang H, Luo Z, Wu K, Tong J, Zhou Z and Lu A 2023 *Opt. Mater.* **135** 113256
- [30] Adamu S B, Halimah M K, Chan K T, Muhammad F D, Nazrin S N and Tafida R A 2022 *J. Lumin.* **250** 119099
- [31] Anthony Raj V, Josuva D' Silva A, Armstrong Arasu K, M M and Rayappan I A 2023 *Physica B* **651** 414590
- [32] Liang H, Liu X, Tong J, He P, Zhou Z, Luo Z and Lu A 2023 *Ceram. Int.* **49** 15266–75
- [33] Kaur S, Pandey O P, Jayasankar C K and Verma N 2022 *Radiat. Phys. Chem.* **199** 110375
- [34] Roopa S and Eraiah B 2021 *J. Non-Cryst. Solids* **551** 120394
- [35] Jha K and Jayasimhadri M 2016 *J. Alloys Compd.* **688** 833–40
- [36] Divina R, Teresa P E and Marimuthu K 2021 *J. Alloys Compd.* **883** 160845
- [37] Mahamuda S, Swapna K, Packiyaraj P, Srinivasa Rao A and Vijaya Prakash G 2013 *Opt. Mater.* **36** 362–71
- [38] Elsaghier H M, Azooz M A, Zidan N A, Abbas W, Okasha A and Marzouk S Y 2022 *Opt. Mater.* **131** 112624
- [39] Zhu L, Zhao D, Li C, Ding J, Li J and Zhou Y 2023 *Ceram. Int.* **49** 12301–8
- [40] Walsh B M 2006 *Advances in Spectroscopy for Lasers and Sensing* ed Di Bartolo B and Forte O (Springer) pp 403–33
- [41] Thabit H A, Ismail A K, Jagannath G, Abdullahi I, Hashim S and Sayyed M I 2023 *J. Non-Cryst. Solids* **608** 122258
- [42] Hussain S et al 2019 *Solid State Commun.* **298** 113632
- [43] Lakshminarayana G, Baki S O, Lira A, Caldiño U, Meza-Rocha A N, Kityk I V, Abas A F, Alresheedi M T and Mahdi M A 2018 *J. Non-Cryst. Solids* **481** 191–201
- [44] Shivani P, Anu K, Sahu A, K M, Rani P R, Deopa N, Punia R and Rao A S 2020 *J. Non-Cryst. Solids* **544** 120187
- [45] Sanju M, Ravina, Anu, Kumar A, Kumar V, Sahu M K, Dahiya S, Deopa N, Punia R and Rao A S 2021 *Opt. Mater.* **114** 110937
- [46] Monisha M, Mazumder N, Melanthota S K, Padasale B, Almuqrin A H, Sayyed M I, Karunakara N and Kamath S D 2022 *Opt. Mater.* **128** 112447
- [47] Kibrıslı O, Ersundu A E and Ersundu M Ç 2019 *J. Non-Cryst. Solids* **513** 125–36
- [48] Chandrappa V, Basavapoornima C, Venkatramu V, Depuru S R, Kaewkhao J, Pecharapa W and Jayasankar C K 2022 *Optik* **266** 169583
- [49] Zheng C, Sun Z, Li W, Yang Y and Mei B 2021 *Mater. Chem. Phys.* **273** 125141
- [50] Ruamnikhom R, Yasaka P, Boonin K, Limsuwan P and Kaewkhao J 2023 *Radiat. Phys. Chem.* **202** 110485
- [51] Biswas J and Jana S 2023 *Opt. Mater.* **141** 113932
- [52] Vijayalakshmi L, Naveen Kumar K and Baek J D 2022 *J. Rare Earths* **42** 46–56